Chemistry & Biology, Vol. 10, 1033–1041, November, 2003, ©2003 Elsevier Science Ltd. All rights reserved. DOI 10.1016/j.chembiol.2003.10.014

Structural Basis for Thrombin Activation of a Protease-Activated Receptor: Inhibition of Intramolecular Liganding

Stacy Seeley,[1,2,4] Lidija Covic,[1,3] Suzanne L. Jacques,[1,3] James Sudmeier,[2] James D. Baleja,[2] and Athan Kuliopulos[1,2,3,*]
[1]Division of Hematology/Oncology and Department of Medicine
[2]Department of Biochemistry
Tufts University School of Medicine
[3]Molecular Cardiology Research Institute
New England Medical Center
Boston, Massachusetts 02111

Summary

Protease-activated G protein-coupled receptors (PAR1–4) are tethered-ligand receptors that are activated by proteolytic cleavage of the extracellular domain (exodomain) of the receptor. PAR1, the prototypic member of the PAR family, is the high-affinity thrombin receptor of platelets and vascular endothelium and plays a critical role in blood coagulation, thrombosis, and inflammation. Here, we describe the solution structure of the thrombin-cleaved exodomain of PAR1. The side chains of a hydrophobic hirudin-like (Hir) sequence and adjacent anionic motif project into solution. Docking of the exodomain Hir sequence to exosite I of thrombin reveals that the tethered ligand in the cleaved exodomain bends away from thrombin, leaving its active site available to another large macromolecular substrate. The N-terminal ligand is longer than anticipated and forms an intramolecular complex with a region located in the C terminus of the exodomain. Mutational analysis confirmed that this C-terminal region is a ligand binding site for both intra- and intermolecular ligands. A lipidated-ligand binding site peptide was found to be an effective inhibitor of thrombin-induced platelet aggregation.

Introduction

The PARs act as exquisite sensors for the presence of extracellular proteases and help the cell respond to the new environment that is being altered during proteolysis. The four different PARs (PAR1, PAR2, PAR3, and PAR4) each respond to a select group of proteases [1, 2]. For example, PAR1 and PAR3 are high-affinity receptors for thrombin [3, 4], PAR2 is activated by tryptase/trypsin [5], and PAR4 is activated by thrombin and trypsin [6]. Thrombin cleavage of PAR1 rapidly activates platelet aggregation and can cause arterial thrombosis under high flow conditions [7, 8]. Chronic stimulation of PAR1 in the prothrombotic milieu of an atherosclerotic plaque has also been implicated in smooth muscle cell proliferation and restenosis [9]. More recently, PAR1 has been shown to be essential for new blood vessel formation during embryogenesis [10] and controls the invasion of epithelial-derived breast cancer cells [11, 12]. Given the importance of PAR1 in thrombotic and proliferative diseases and the unique difficulty of blocking a tethered-ligand receptor [13], considerable effort has been expended to generate PAR1 antagonists, including antibodies [14], ligand-based small molecules [15, 16], and cell-penetrating pepducins that prevent PAR1 from signaling to internally located G proteins [17, 18].

Thrombin [3] and other proteases such as plasmin [19] activate PAR1 by cleaving its exodomain at the Arg 41-Ser 42 peptide bond. The new N terminus that is generated activates transmembrane signaling by a poorly understood intramolecular liganding mechanism. The cleaved exodomain is flexible and can reach over and activate an adjacent receptor on the same membrane surface [20, 21]. Synthetic peptides of five or more amino acids can also activate PAR1 in an intermolecular liganding mode [22]. A number of mutagenesis studies have been conducted [23–26] that aimed at delineating the inter- and intramolecular interactions between PAR1 and its peptide ligands. As with the other members of the polypeptide-ligand class of GPCRs [27], it was anticipated that the ligand binding sites would include regions in both the N-terminal exodomain (e1) and hydrophilic extracellular loops e2–e4 (for simplicity, we have referred to extracellular loops ECL1–ECL3 as e2–e4, respectively). Indeed, extracellular domain/loop swapping experiments using human/*Xenopus* PAR1 chimeras [28] and PAR1/PAR2 chimeras [29] led to the broad conclusion that ligand binding determinants were potentially present on extracellular domain e1 and loops e2–e4. Likewise, mutations in the e3 loop of PAR2 caused deficiencies in both intra- and intermolecular liganding [30, 31]. In other studies [24–26, 30], an emphasis was placed on mutating extracellular anionic residues in the hope of identifying an appropriate partner(s) to the cationic moieties on the ligand. Mutation of e3 residue E^{260} to Arg complemented the charge-reversed peptide ligand, SFLLRN→SFLLEN, strongly suggesting that E^{260} forms a salt bridge to R^{46} in PAR1 [25]. Alanine substitution of all extracellular Glu and Asp residues including E^{260} showed that only mutation of e3 residue D^{256} and e4 residue E^{347} significantly affected activation by intra- and intermolecular ligands [26]. However, these mutations had little or no effect on the affinity of radioligands for PAR1, which cast doubt upon whether these residues provide actual ligand binding contact(s). Moreover, the recent X-ray structure of rhodopsin [32] places the D^{256} residue in a conserved β sheet located deep within the hydrophobic core of the extracellular loops where it is likely to be completely inaccessible to peptide ligand in the context of PAR1. Therefore, a limitation of mutagenesis is that by itself it cannot distinguish between direct versus indirect effects on ligand binding.

In addition to containing the tethered ligand, the PAR1 exodomain also harbors a hirudin-like (Hir) sequence element [33], K^{51}YEPF^{55}, that is essential for high-affinity

*Correspondence: athan.kuliopulos@tufts.edu
[4] Present Address: Department of Science and Mathematics, Kettering University, Flint, Michigan.

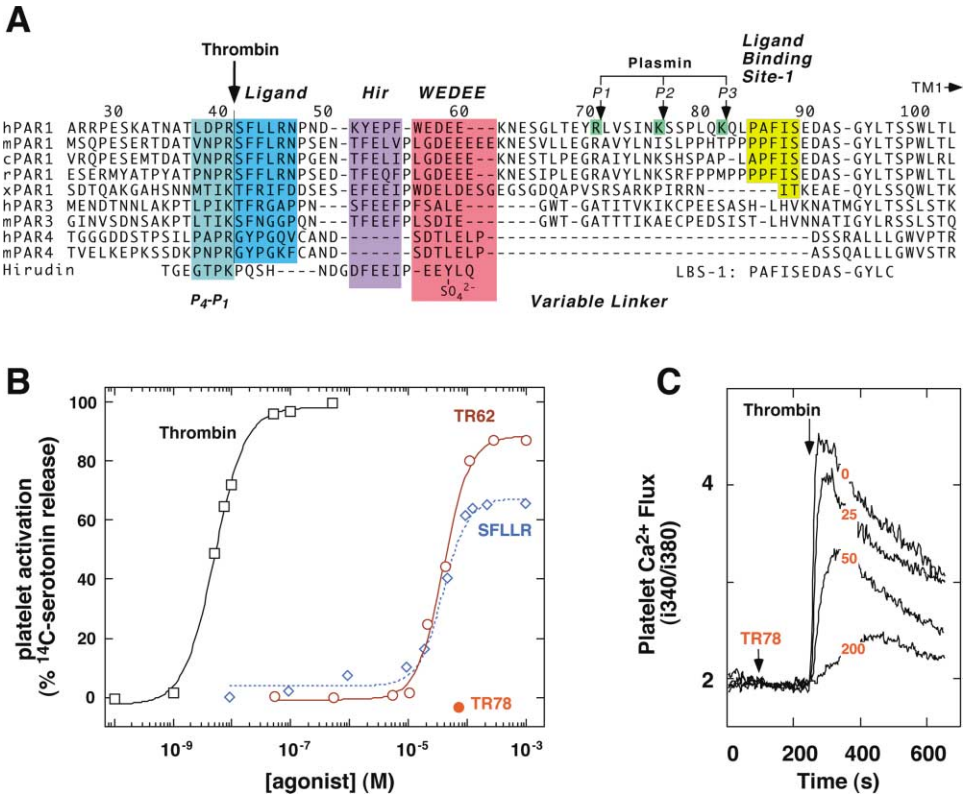

Figure 1. Biological Activities of the Full-Length TR78 and Thrombin-Activated TR62 Extracellular Domains of PAR1

(A) Alignment of thrombin receptor exodomains from human (h), mouse (m), hamster (c), rat (r), and *Xenopus* (x) with the C terminus of the leech anticoagulant protein, hirudin. Thrombin cleaves the TR78 exodomain after R^{41} to generate TR62 (S^{42}-hSer^{103}). Plasmin cleaves the exodomains at the P1–P3 sites located in the flexible linker that separates the ligand from the ligand binding site-1. TM1 indicates the predicted start of the first transmembrane α helix.

(B) Activation of human platelets by thrombin, TR62, and SFLLR. The data were fit to a one-site equation y = (m1 − m2/(1 + ([agonist]/EC_{50}^{n})) + m2) by nonlinear regression analysis using Kaleidagraph 3.05, where n is the hill coefficient and m1 and m2 are the minimum and maximum asymptotes, respectively.

(C) TR78 (μM concentrations indicated on each trace) inhibits 3 nM thrombin-dependent Ca^{2+} fluxes in human platelets. Intracellular Ca^{2+} fluxes were monitored as the ratio of fluorescence excitation intensities at 340/380 nm as described in Experimental Proceduers.

interactions with thrombin [34–36]. X-ray crystallographic analyses of thrombin complexed with short PAR1 exodomain peptides comprising Leu 38 to Ser 64 showed that the Hir sequence of PAR1 bound to exosite I of thrombin [37]. However, under the conditions of crystallization, the PAR1 peptides adopted an unusual antiparallel β sheet structure sandwiched between two thrombin molecules. In this structure, the Hir sequence docked in the expected manner at exosite I of one thrombin molecule, but the PAR1 cleavage sequence bound in a nonproductive mode with the active site of an adjacent thrombin molecule. The physiological significance for this unexpected thrombin:PAR1:thrombin binding mode remains to be identified.

Steady-state kinetic studies using soluble full-length PAR1 exodomains showed that the initial binding of the Hir sequence of PAR1 with exosite I is essential for rapid association to thrombin [38]. In a second and rate-limiting step, the exosite I-bound Hir motif facilitates the productive interaction of the PAR1 cleavage sequence to the active site of thrombin. The subsequent irreversible steps of peptide bond cleavage are rapid and allosterically enhanced by the presence of the docked Hir sequence. Following cleavage, thrombin remains associated with the C-terminal portion of the PAR1 exodomain via this high-affinity Hir sequence [38]. Complementary studies with an array of thrombin active site and exosite mutants further demonstrated the importance of the thrombin exosite I for efficient binding and cleavage of PAR1 peptides [39].

Here, we determine the NMR structure of the thrombin-cleaved PAR1 exodomain. Docking of the PAR1 exodomain Hir motif to exosite I of thrombin reveals that the active site of thrombin is readily accessible to another large macromolecular substrate. This supports the notion that an additional role of the PAR1 Hir sequence is to tether thrombin to the platelet surface and assist in the cleavage of other nearby platelet receptors that lack a high-affinity Hir-like sequence. The N-terminal tethered ligand forms an intramolecular complex with a region located in the C terminus of the PAR1 exodomain that was confirmed to be an authentic ligand binding site in full-length receptor. Thus, a lipidated ligand binding site peptide, P^{85}AFISEDASGYL^{96}C-(p-maleimidophe-

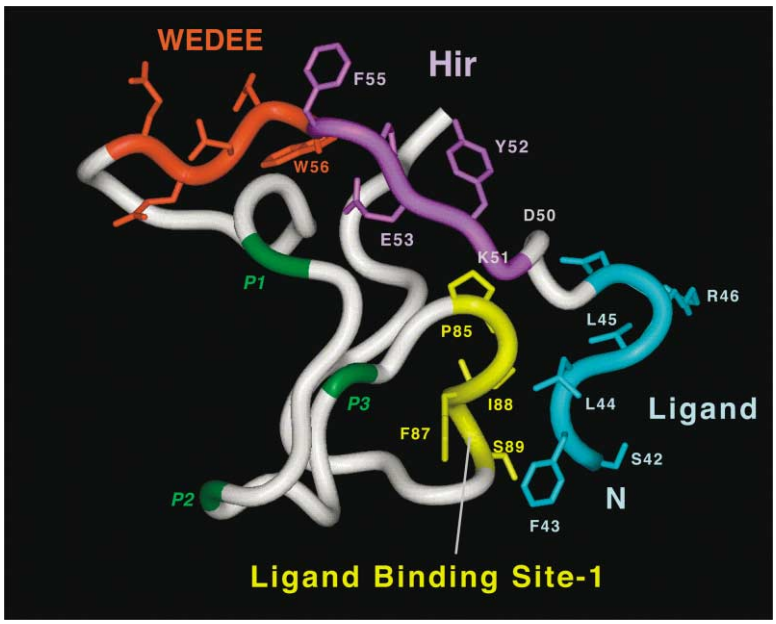

Figure 2. Solution Structure of the Thrombin-Activated PAR1 Exodomain, TR62, Residues 42–103

The rmsd for the mean coordinate positions was 1.9 ± 0.4 Å for residues 43–51 and 85–89 and 2.3 ± 0.4 Å for residues 52–56 and 62–69 for the backbone atoms (N, Cα, C′) of an ensemble of the best ten structures (see Supplemental Table S1 at *Chemistry & Biology*'s website). No distance restraint was violated by more than 0.2 Å, and no torsional restraint was violated by more than 5°. The total energy was −251 ± 31 kcal mol^{-1}, and the van der Waals energy was −319 ± 16 kcal mol^{-1}. P1–P3 indicate the three plasmin cleavage sites located on the flexible linker separating the anionic WEDEE motif from ligand binding site-1.

nyl-butyramide)-phosphoethanolamine(dipalmitoyl), could completely block aggregation of human platelets induced by thrombin.

Results and Discussion

Structure of the Thrombin-Cleaved PAR1 Exodomain

Previous studies demonstrated that the N-terminal exodomain of PAR1 (Figure 1A) contains all of the determinants for thrombin recognition and cleavage [36]. In *E. coli* [19], we produced a soluble version of the PAR1 exodomain, residues A^{26}-homoSer^{103} (TR78), which has high affinity (K_{is} = 2.4 μM) for thrombin [38]. Cleavage with 10 nM thrombin yielded the C-terminal fragment, residues S^{42}-hS^{103} (TR62). The TR62 exodomain is able to fully activate human platelets with EC_{50} of 40 μM, similar to activation of PAR1 with SFLLR, a peptide derived from the N terminus of TR62 (Figure 1B). The full-length exodomain, TR78, does not activate platelets (Figure 1B) but is able to inhibit thrombin-dependent Ca^{2+} fluxes with IC_{50} of 50 μM (Figure 1C), most likely because it can directly compete for platelet PAR1 as a thrombin substrate [19].

The thrombin-cleaved exodomain, TR62, exhibited much higher solubility than TR78 for the extended times required for NMR data acquisition while retaining biological activity; therefore, we chose TR62 for structural determination. As a reflection of its biological function, the TR62 exodomain was flexible but had obvious tertiary structure because of the observations of nuclear Overhauser effect (NOE) crosspeaks between Trp 56 and methyl resonances from aliphatic residues distant in the sequence. The N- and C-terminal regions of the TR62 exodomain are the most structured and are separated by a flexible linker comprising residues Arg 70 to Lys 82 (Figure 2).

The most striking structural feature is that the N-terminal S^{42}FLLRNPNDK^{51} tethered ligand docks onto the surface of C-terminal residues P^{85}AFIS^{89}, a region which we have termed ligand binding site-1 (LBS-1). Mutagenesis studies previously identified a similar region as an essential receptor-activation motif [24]. As shown in Figure 2, the aromatic ring of ligand residue Phe 43 comes into van der Waals contact with the side chain of Ser 89 which projects from the end of LBS-1. Eight NOEs were observed between Phe 43 and Ser 89, demonstrating an extensive intramolecular interaction. Because of the relatively dynamic nature of the structure, we cannot determine the occupancy of any particular NOE interaction and cannot rule out an NOE being transient. However, mutation of Phe 43 to Ala abrogates intramolecular receptor activation [20], and the S89A mutant displays a 23- to 60-fold loss in activity to small peptide agonists [25, 26]. The adjacent LBS-1 Ile 88 residue forms hydrophobic contacts with ligand residue Leu 44, and mutation of Ile 88 to Ala causes a 40- to 60-fold loss in peptide agonist activity [25, 26]. The aromatic ring of Phe 87 and the anionic residues at the C-terminal side of LBS-1, Glu 90, and Asp 91 do not come into contact with the ligand; accordingly, mutation of these residues to Ala had little or no effect on receptor activation [24–26]. Likewise, the N-terminal α-amino group of Ser 42 does not come into contact with LBS-1. A free N-terminal amino group is not strictly necessary for agonist activity and is absent in the antagonist, BMS-200661 (K_d = 20 nM) [15], which has a bulky *N*-trans-cinnamoyl group in place of the N-terminal serine. However, substitutions of the aryl moiety of the cinnamoyl group indicated a high degree of structural specificity. Therefore, it is likely that the extreme N terminus of the ligand fits into a binding pocket defined by other e2–e4 residues which can accommodate both the cationic N-terminal Ser 42 and the larger, neutral, cinnamoyl group of BMS-200661.

An unexpected interaction was found between Pro 85-Ala 86 and the peptide backbone of Asp 50-Lys 51 (Figure 2), revealing that the intramolecular ligand is considerably longer than was predicted by structure-function studies [22, 40]. It is also noteworthy that the ligand forms a tight turn about Arg 46 whose guanidino group projects away from LBS-1. Interestingly, cyclic peptide ligands such as cyclo(Phe-Leu-Leu-Arg-ϵLys) which are bent at the analogous Arg 46 position are potent agonists of PAR1 [41]. Therefore, it is possible that a bent conformation may also occur with linear intermolecular agonists such as SFLLRN. In addition, mutation of Arg 46 to Ala causes a 33-fold loss in activity in the context of small peptide agonists [22], and the guanidino group is an important phamacophore for small molecule anti-PAR1 compounds [15]. Thus, it is likely that yet another region or regions [25] of the extracellular loops (e2–e4) of PAR1 will provide further ligand binding surfaces for this cationic moiety, potentially as a second event in a two-step liganding process. In a potentially analogous mechanism, the glycoprotein hormone GPCRs are activated in two steps whereby the glycoprotein ligand (LH, FSH, CG, TSH) first binds with high affinity to the N-terminal e1 domain of the receptor and then makes secondary contacts with the other extracellular loops to generate a signal [27].

The NMR structure of the PAR1 exodomain also shows that the thrombin-interacting Hir sequence, $Y^{52}EPF^{55}$, extends directly away from the ligand region (Figure 2). Loss of this Hir motif causes a 73-fold reduction in the association rate of thrombin to the exodomain [38], and individual mutation of Tyr 52, Glu 53, or Phe 55 to Ala causes up to a 50-fold loss in the ability of thrombin to activate full-length receptor [35]. The aromatic side chains of Tyr 52 and Phe 55, along with Glu 53, project into solution where they are easily accessible for forming interactions with exosite I of thrombin (see Figure 5). Adjacent to the Hir motif is an anionic $E^{57}DEE^{60}$ cluster that splays outward from the exodomain where it is available for electrostatic interactions with the positively charged thrombin exosite-1 [33]. A hydrophobic scaffolding residue, Trp 56, anchors both the adjacent Hir and EEDE motifs by making numerous contacts (n = 28 NOEs) with Pro 54, Phe 55, Glu 57, Asp 58, Leu 66, and Thr 67. Kinetic analyses of soluble PAR1 exodomains showed that the presence of Trp 56 enhances the affinity of the adjacent Hir sequence for exosite I of thrombin by 11-fold [42]. The R^{70}-K^{82} linker region joining the EDEE motif to LBS-1 is likely to be the most dynamic portion of TR62, as indicated by the relatively low number of NOE interactions within this segment and the absence of NOEs to other parts of the protein (see Supplemental Figure S1 at http://www.chembiol.com/cgi/content/full/10/11/1033/DC1). This is the region that is efficiently cleaved by plasmin [19] at the P1-P3 sites (Figures 1A and 2). We postulate that this linker serves dual purposes: (1) it provides sufficient conformational flexibility for the exodomain N-terminal ligand to achieve the correct geometry necessary to reach the ligand binding site, and (2) its flexibility allows for truncation by serum proteases such as plasmin by a negative feedback mechanism during the anticoagulation phase of hemostasis [19].

Intra- and Intermolecular Liganding

To help identify conformational changes that may take place following exodomain cleavage by thrombin, we compared the chemical shift patterns of the peptide backbone ^{1}H-^{15}N HSQC crosspeaks arising from TR62 with those of the uncleaved exodomain, TR78 (Figure 3A). The HSQC spectra of the two exodomains are highly superimposable, with the important exception of the tethered ligand region, which indicates that the overall structures of the cleaved and uncleaved exodomains are quite similar. The ^{1}H-^{15}N crosspeaks from ligand residues Leu 44, Leu 45, Arg 46, and Asn 47 gave shifts much larger than that expected from simply breaking the Arg 41-Ser 42 peptide bond [43], indicating that the structure of the ligand region in the thrombin-cleaved exodomain is quite different from that of uncleaved exodomain. Smaller shifts were seen in the HSQC crosspeaks arising from Hir residues Tyr 52, Glu 53, and Phe 55 of TR62 versus TR78. Therefore, the Hir region may slightly change its conformation following thrombin cleavage [38] and intramolecular liganding. The crosspeaks arising from LBS-1 residues were superimposable in TR62 and TR78. In addition, no NOE interactions were detected between the ligand region and LBS-1 in TR78 (data not shown). This indicates that the Ala 26-Arg 41 N-terminal extension present in the uncleaved exodomain may disrupt intramolecular liganding by changing the structure of the tethered ligand rather than the ligand binding site. Note that differences in chemical shifts illustrate a change in environment, such as one caused by a conformational change, but a structural difference can only be confirmed by solving the structure of the larger TR78.

The intramolecular liganding between the N-terminal residues of TR62 and the LBS-1 region was further demonstrated by competition titration NMR studies of TR62 with free peptide ligand. As shown in Figure 3B, addition of SFLLRN caused selective shifts in the ^{1}H-^{15}N crosspeaks of ligand residues Leu 44, Leu 45, and Arg 46 in TR62. Nearly identical results were seen with the high-affinity BMS-200661 PAR1-antagonist (data not shown). This provides the first direct evidence that small peptide ligands and antagonists can displace the tethered ligand from LBS-1 in the TR62 exodomain, as occurs with the thrombin-cleaved receptor on intact cells [16, 44]. As expected, addition of SFLLRN (Figure 3C) or BMS-200661 (data not shown) to TR78 caused no movement of the ^{1}H-^{15}N crosspeaks of the preligand region, providing further evidence that the preligand does not form an intramolecular complex with the ligand binding site in the uncleaved PAR1 exodomain.

To further test the validity of the structure of the soluble exodomain as a model for full-length receptor, we deleted the $P^{85}AFIS^{89}$ region, expressed the $\Delta P^{85}AFIS^{89}$ mutant receptor in COS7 fibroblasts, and measured PAR1-dependent stimulation of PLC-β. As shown in Figure 4A, the EC_{50} for SFLLRN stimulation of PLC-β shifted $\sim$13,000-fold for ΔPAFIS relative to wild-type receptor. The $\Delta P^{85}AFIS^{89}$ mutation also caused a 73-fold shift in EC_{50} for thrombin and reduced efficacy by 2.5-fold. It is unlikely that this right shift in EC_{50} is due to a lower affinity for thrombin, because previous studies showed that deletion of the C terminus of the exodomain includ-

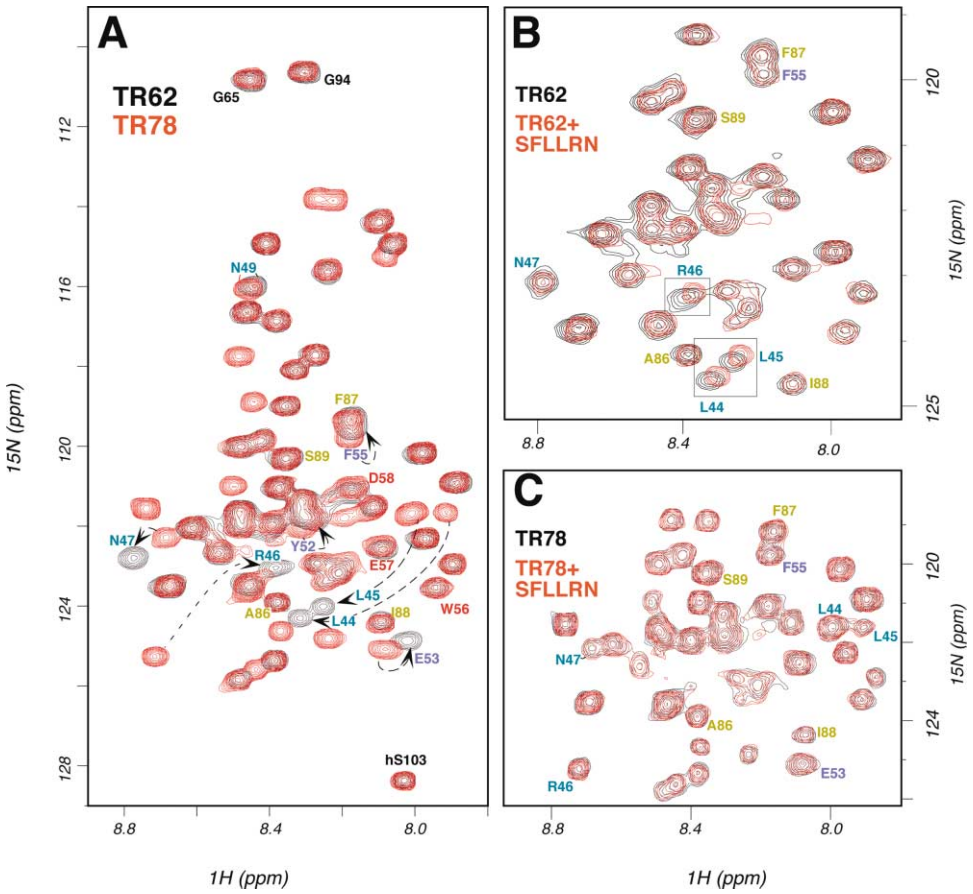

Figure 3. Movement of the Ligand Region of the PAR1 Exodomain Following Thrombin Cleavage or upon Displacement by the Small Peptide Ligand, SFLLRN

(A) Superposition of $^{1}H/^{15}N$ HSQC spectra of full-length TR78 (1.4 mM) and thrombin-cleaved TR62 (1.6 mM) in 20 mM sodium phosphate (pH 7.2), 5% D_2O, 5°C. Selected $^{1}H/^{15}N$ crosspeaks are labeled in blue (ligand), purple (Hir), red (WEDEE), and yellow (ligand binding site-1).

(B) Overlay of $^{1}H/^{15}N$ HSQC spectra of TR62 (1.6 mM) and TR62 (0.93 mM) in the presence of SFLLRN ligand (2.76 mM). Boxed crosspeaks highlight the only differences in the two spectra occurring in the ligand region of TR62.

(C) Overlay of $^{1}H/^{15}N$ HSQC spectra of TR78 (0.88 mM) and TR78 (0.8 mM) in the presence of SFLLRN ligand (2.4 mM).

ing the LBS-1 region [38] produced a 2-fold higher affinity for thrombin compared to the full-length exodomain. Likewise, deleterious mutations in intracellular loops can cause right shifts in the EC_{50} for the thrombin-generated tethered ligand [17]. Therefore, the most likely explanation for the right shift in thrombin EC_{50} by the LBS-1 mutant is that a greater fraction of receptors needs to be cleaved in order to generate a signal. The severe defects in receptor activation strongly support the NMR data that the $P^{85}AFIS^{89}$ LBS-1 region is a major binding site for both intra- and intermolecular ligands. The residual activity of the $\Delta P^{85}AFIS^{89}$ mutant at saturating concentrations of thrombin and SFLLRN is likely due to the presence of other ligand binding regions from the extracellular loops e2–e4, as previously described for PAR1 [25, 26] and PAR2 [31].

Ligand Binding Site-1 Peptide Antagonists

Previous studies [45] demonstrated that soluble extracellular loop fragments of the V_{1a} vasopressin receptor are low micromolar inhibitors of vasopressin binding. These studies suggested that the peptides (13–25-mers) mimic the extracellular loops of the intact receptor and may either bind to the ligand or indirectly perturb the ligand binding pocket. Therefore, using the structure of the cleaved exodomain as a starting point, we tested whether a peptide fragment comprising LBS-1 residues P^{85}-$L^{96}C$ could inhibit intramolecular liganding of PAR1 on human platelets. The LBS-1 peptide did inhibit platelet Ca^{2+} fluxes generated by 3 nM thrombin (Figure 4B) or by 3 μM SFLLRN (data not shown). However, the IC_{50} (120 μM) was relatively weak, and concentrations of LBS-1 peptide up to 120 μM did not inhibit thrombin-induced platelet aggregation (Figure 4C). Other exodomain peptides, A^{26}-R^{41} and T^{67}-L^{84} (1–300 μM), did not inhibit thrombin or SFLLRN activation of PAR1 (data not shown). To enhance effective molarity at the platelet surface and reduce degrees of freedom, we attached a lipid moiety (dipalmitoyl-phosphoethanolamine) to a C-terminal cysteine, a position on the LBS-1 peptide that was predicted to come into close proximity with the lipid bilayer in the intact receptor (see Figure 5). In marked contrast to the soluble LBS-1 peptide, the C terminally lipidated peptide, LBS1-PE, was a highly ef-

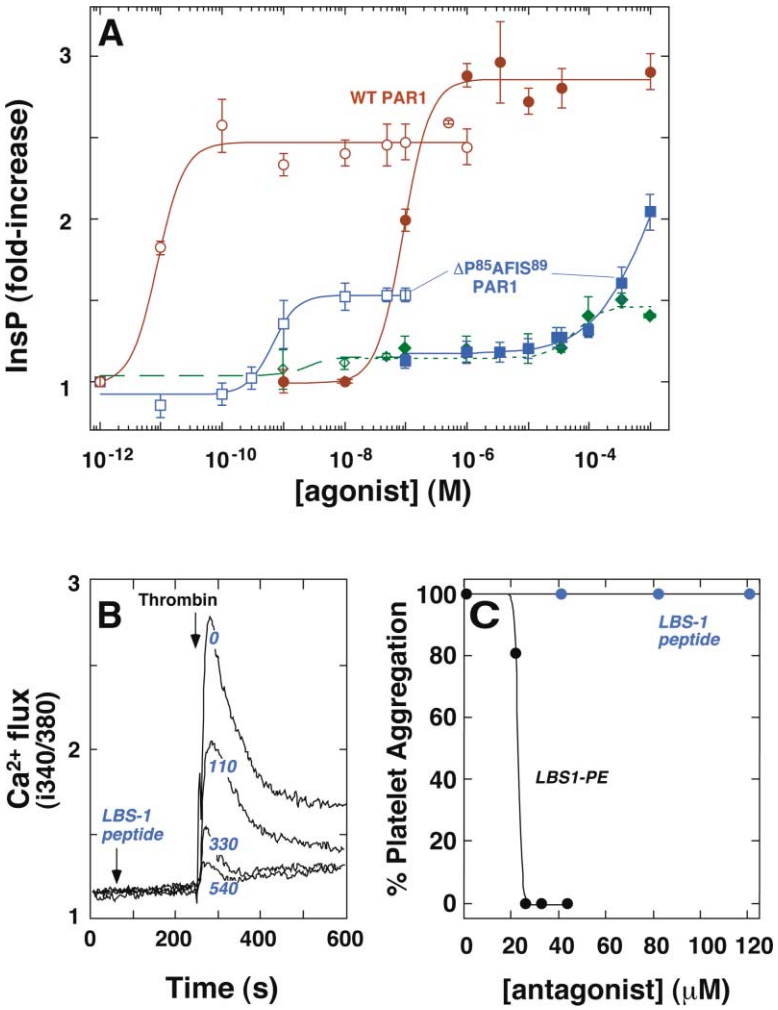

Figure 4. The $P^{85}AFIS^{89}$ Region of PAR1 Is a Ligand Binding Site for Both the Tethered and Free Peptide Ligand, SFLLRN

(A) Effect of deletion of $P^{85}AFIS^{89}$ on the ability of PAR1 to signal to PLC-β in fibroblasts. COS7 cells were transiently transfected with pDEF3 vector encoding wild-type PAR1 (brown circles), $\Delta P^{85}AFIS^{89}$ PAR1 (blue squares), or empty vector (green diamonds) and challenged with 1 pM to 1 μM thrombin (open symbols) or 1 nM to 1 mM SFLLRN peptide (closed symbols). The $\Delta P^{85}AFIS^{89}$ mutant was expressed equally as well as wild-type PAR1 as assessed by flow cytometry with the anti-SFLLR Ab [19]. PLC-β activity was determined by measuring total [^{3}H]inositol phosphate (InsP) formation, and the data were fit as in Figure 1B.

(B) The LBS-1 peptide ($P^{85}AFISEDASGYL^{96}$-C) spanning the ligand binding site-1 region (Figure 1A) inhibits thrombin activation of human platelets. Gel-filtered platelets were preincubated with the indicated concentrations of LBS-1 peptide (110–540 μM) and then challenged with 3 nM thrombin. Intracellular Ca^{2+} fluxes were measured as in Figure 1C. The LBS-1 peptide was not a direct thrombin inhibitor at concentrations up to 300 μM as assessed by competition studies with small chromogenic substrates [38].

(C) Effect of C-terminal lipidation of the LBS-1 peptide with dipalmitoyl-phosphoethanolamine (LBS1-PE) on antagonism of thrombin-induced platelet aggregation. Gel-filtered human platelets were pretreated for 5 min with either soluble LBS-1 or LBS1-PE, and aggregation was induced with 5 nM thrombin.

fective inhibitor of platelet aggregation. As shown in Figure 4C, 23 μM LBS1-PE completely inhibited 5 nM thrombin-induced platelet aggregation. Similarly lipidated extracellular loop peptides such as KEQTIQVP GLNITTC(dipalmitoyl-phosphoethanolamine)HDVL NETLLEGY had no effect on platelet aggregation at concentrations up to 50 μM (data not shown). Therefore, anchoring a ligand binding site peptide to the cell surface with a lipid moiety at the appropriate position may interfere with agonist binding either by directly interacting with the ligand or by binding to the receptor itself and altering the ligand binding pocket [45].

Docking of Thrombin to the PAR1 Exodomain

An interesting feature of thrombin-PAR interactions on platelets is that near-stoichiometric amounts of thrombin, rather than catalytic amounts, are required for platelet activation [46]. This raises the possibility that the low turnover of thrombin could be due to tight binding and a relatively slow off-rate from cleaved receptors. Indeed, previous kinetic studies [38] demonstrated that the Hir region of TR62 confers high-affinity binding (K_i = 9.4 μM) of thrombin-cleaved exodomain to thrombin. To provide a model of this complex, we docked the NMR-based structure of TR62 onto the surface of thrombin by superimposing the side chains of the three critical Hir residues, Tyr 52, Glu 53, and Phe 55, with the analogous residues of hirulog-3 bound to thrombin [47]. Notably, the model of the TR62-thrombin complex (Figure 5) shows that the N-terminal ligand bends away from the surface of thrombin in order to form the intramolecular contacts with the LBS-1 region of the PAR1 exodomain. This is consistent with the conformational change in the ligand region following cleavage of the full-length exodomain by thrombin (Figure 3A). This more open geometry is in marked contrast to the three-stranded β sheet PAR1 structure observed in the thrombin-PAR1(L^{38}-E^{60})-thrombin cocrystal [37]. The PAR1 exodomain-thrombin model in Figure 5 leaves the active site of thrombin free to simultaneously interact with other large macromolecules, such as the lower affinity PAR4 receptor, which lacks a Hir-like sequence [42]. This accessible active site is interesting in light of recent studies that have shown that mouse PAR3 serves as a Hir-containing thrombin binding site that assists in the cleavage of adjacent PAR4 receptors [48]. Although the analogous cofactoring between PAR1 and PAR4 has yet to be shown, our model provides a mechanistic basis

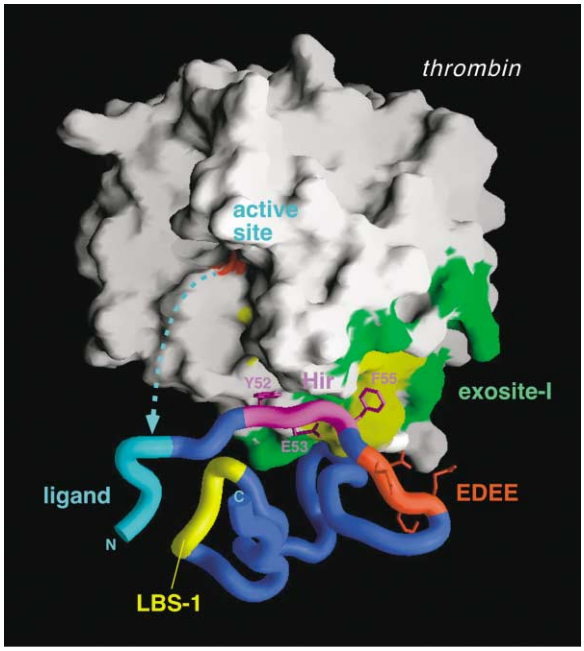

Figure 5. Model of the PAR1 Exodomain, TR62, Complexed with Thrombin

The amino acid residues on thrombin are colored as follows: red, Ser 195; green, Lys 36, Arg 67, Arg 75, Arg 77a, Lys 81, Lys 109, Lys 110; and yellow, Leu 40, Leu 65, Tyr 76, Ile 82.

for cofactoring that might occur between high-affinity (PAR1, PAR3) and low-affinity (PAR4) thrombin receptors [48].

Significance

The protease-activated receptors, PAR1, PAR2, and PAR4, play a major role in blood coagulation and in mediating the cellular responses to injury and inflammation in many tissues. More recently, PAR1 has been shown to be an oncogene that controls the invasion and metastasis of cancer cells. There has been a concerted effort by the pharmaceutical industry to develop anti-PAR drugs; however, these efforts have been largely thwarted due to the difficulty of antagonizing receptors that form intramolecular complexes with their own ligand. Here, we determine the structural basis for proteolytic activation of the prototypic PAR1 thrombin receptor and lay the foundation toward the development of more effective anti-PAR small molecules. NMR experiments indicate that following cleavage by thrombin the PAR1 exodomain undergoes a major conformational change in the ligand region and a smaller conformational change in the thrombin exosite I binding Hir residues. Docking of the exodomain Hir sequence to exosite I of thrombin revealed that the tethered ligand in the cleaved exodomain bends away from thrombin, leaving the thrombin active site available to another large macromolecular substrate. The N-terminal ligand forms an intramolecular complex with the LBS-1 region ($P^{85}AFIS^{89}$) located in the C terminus of the exodomain. The ligand region is longer than anticipated and includes peptide backbone contacts between Asp 50-Lys 51 and Pro 85-Ala 86. Unlike a soluble LBS-1 peptide, a lipidated LBS-1 peptide, $P^{85}AFISEDASGYL^{96}$C-(p-maleimidophenyl-butyramide)-phosphoethanolamine(dipalmitoyl), could completely block aggregation of human platelets induced by 5 nM thrombin. Thus, anchoring a ligand binding site peptide to the cell surface with a lipid moiety at the appropriate position may either create a competing binding site for the ligand or perturb the ligand binding pocket of the intact receptor and block receptor activation.

Experimental Procedures

NMR Sample Preparation

Full-length PAR1 exodomain, TR78, was expressed from *Escherichia coli* as a KSI-M-TR78-M-His_6 fusion protein and purified by Ni chelate chromatography using the pET31 vector [49]. TR78 was cleaved at interspersed methionines from KSI carrier protein and His_6 tag using CNBr/70% formic acid and purified by RP-HPLC as described [19]. TR62 was made by incubating 200–400 μM TR78 with 10 nM thrombin at 25°C for 1 hr. The C-terminal exodomain, TR62, was purified from the N-terminal TR16 cleavage fragment (A^{26}-R^{41}) by RP-HPLC and reconstituted in 20 mM $NaHPO_4$, 150 mM NaCl (PBS) (pH 7.2). Uniformly ^{15}N-labeled protein was prepared by growing cells in M9 medium supplemented with $^{15}NH_4Cl$. NMR samples contained 0.6–1.6 mM exodomain.

NMR Structure Determination

NMR spectra were collected at 5°C on a Bruker 500 MHz spectrometer. ^1H and ^{15}N resonances were assigned from two- and three-dimensional TOCSY and TOCSY-HSQC experiments. Distance restraints were obtained from two-and three- dimensional NOESY and NOESY-HSQC experiments, and ϕ-angle restraints were based on the $^3J_{HNH\alpha}$ coupling constants. Structures of TR62 were calculated with a square-well potential and force constant of 50 $kcal^{-1}\,mol^{-1}\,Å^{-2}$ by distance geometry/simulated annealing algorithms using the X-PLOR program [50].

Molecular Modeling

The NMR-derived structure of TR62 was docked onto the surface of thrombin using the X-ray structural coordinates of the thrombin-hirulog-3 complex [47] as a model. Energy minimization was performed to eliminate van der Waals violations and resulted in a rmsd of 0.8 Å between the atomic coordinates of thrombin complexed with hirulog-3 versus thrombin complexed with TR62 and a rmsd of 1.4 Å between the original atomic coordinates of uncomplexed TR62 and docked TR62. Energy minimization did not alter any significant structural features, with the major movement in the peptide backbone of TR62 occurring in the flexible linker residues R^{70}-K^{82}.

Synthesis of LBS1-PE

The LBS-1 peptide included a C-terminal cysteine residue ($P^{85}AFISEDASGYL^{96}$-C) and was synthesized by solid-phase fmoc chemistry. Lipidation of the C-terminal cysteine thiol of LBS-1 was done with *N*-MPB-PE (1,2-dipalmitoyl-sn-glycero-3-phosphoethanolamine-*N*-[4-(p-maleimidophenyl)-butyramide]) by mixing 2.5 mM peptide and 5 mM *N*-MPB-PE (Avanti Polar Lipids) in 6% triethylamine/17% H_2O/77% dimethylformamide and incubating at 23°C for 2 hr. The LBS-1 peptide-Cys-PE conjugate was purified by Sep-Pak (Waters) C_{18} reverse-phase chromatography, and identity was confirmed by mass spectrometry.

Inositol Phosphate Assay

Accumulation of [^{3}H]inositol phosphates was measured in the presence of 20 mM LiCl. COS7 cells were split into 12-well plates at 200,000 cells/well. [^{3}H]-labeled myoinositol (2 μCi/ml) was added to cells 24 hr prior to the experiment. Wells were rinsed twice with 2

ml DME containing 10 mM HEPES buffer (pH 7.3), then rinsed twice with 2 ml PBS containing 20 mM LiCl. Cells were stimulated with agonist for 30 min and then extracted with cold methanol and chloroform. Extracts were loaded onto columns containing 1 ml anion-exchange resin AG1X8, formate form, 100–200 mesh size (Bio-Rad Laboratories, Cambridge, MA). After loading, columns were washed twice with 10 ml H_2O and twice with 10 ml 60 mM ammonium formate/5 mM Borax. Column fractions were eluted with 4 ml 2 M ammonium formate/0.1 M formic acid into vials containing 7.5 ml scintillation cocktail and counted. The mean of triplicate determinations was expressed as fold-stimulation above nonstimulated cells.

Platelet Aggregation and Ca^{2+} Flux Measurements

Human platelets were obtained from adult volunteers using informed consent procedures approved by the Tufts-NEMC Institutional Review Board. Blood was collected into a 30 ml syringe containing 10% Na citrate as anticoagulant using an 18G needle. Platelets were purified by gel filtration, and activation was measured by ^{14}C-serotonin release [51] following challenge with agonist. For Ca^{2+} signaling assays, platelets were labeled with 2.5 μM Fura 2-AM (Molecular Probes) for 30 min at 37°C. Platelets were then washed and resuspended with an equal volume of modified PIPES buffer. Ca^{2+}/Fura-2 fluorescence was measured as previously [46] using a Perkin Elmer LS50B fluorescence spectrophotometer. For platelet aggregation measurements, isolated platelets were counted on a Coulter counter, and the concentration was adjusted to 1.5×10^8/ml with modified PIPES buffer. Platelet aggregation was measured by light scattering of stirred platelets (900 rpm) at 37°C on a Chronolog 560VS/490-2D aggregometer using modified PIPES buffer as a blank. Platelet samples (250 μl) were preincubated at 37°C with 1.5 mM $CaCl_2$ and treated with LBS-1 or LBS1-PE (dissolved in 50% DMF/50% DMSO) for 5 min before the addition of human α-thrombin (Haematologic Technologies Inc., Essex Junction, VT). Percent aggregation was determined from the extent of aggregation at 5 min.

Acknowledgments

This work was supported by an ASH Fellow Scholar Award to S.L.J. and a Scholar Award from the PEW Charitable Trusts and N.I.H. grants HL57905 and HL64701 to A.K.

Received: July 1, 2003
Revised: August 20, 2003
Accepted: August 20, 2003
Published: November 21, 2003

References

1. Coughlin, S.R. (2000). Thrombin signalling and protease-activated receptors. Nature *407*, 258–264.
2. Hollenberg, M.D., and Compton, S.J. (2002). Proteinase-activated receptors. Pharmacol. Rev. *54*, 203–217.
3. Vu, T.-K.H., Hung, D.T., Wheaton, V.I., and Coughlin, S.R. (1991). Molecular cloning of a functional thrombin receptor reveals a novel proteolytic mechanism of receptor action. Cell *64*, 1057–1068.
4. Ishihara, H., Connolly, A.J., Zeng, D., Kahn, M.L., Zheng, Y.W., Timmons, C., Tram, T., and Coughlin, S.R. (1997). Protease-activated receptor 3 is a second thrombin receptor in humans. Nature *386*, 502–506.
5. Cenac, N., Coelho, A.-M., Nguyen, C., Compton, S., Andrade-Gordon, P., MacNaughton, W.K., Wallace, J.L., Hollenberg, M.D., Bunnett, N.W., Garcia-Villar, R., et al. (2002). Induction of intestinal inflammation in mouse by activation of proteinase-activated receptor-2. Am. J. Pathol. *161*, 1903–1915.
6. Xu, W.-F., Andersen, H., Whitmore, T.E., Presnell, S.R., Yee, D.P., Ching, A., Gilbert, T., Davie, E.W., and Foster, D.C. (1998). Cloning and characterization of human protease-activated receptor 4. Proc. Natl. Acad. Sci. USA *95*, 6642–6646.
7. Andrade-Gordon, P., Derian, C.K., Maryanoff, B.E., Zhang, H.-C., Addo, M.F., Cheung, W.-M., Damiano, B.P., D'Andrea, M.R., Darrow, A.L., DeGaravilla, L., et al. (2001). Administration of a potent antagonist of protease-activated receptor-1 (PAR-1) attenuates vascular restenosis following balloon angioplasty in rats. J. Pharmacol. Exp. Ther. *298*, 34–42.
8. Bahou, W.H. (2002). Attacked from within, blood thins. Nat. Med. *8*, 1082–1083.
9. Nelken, N.A., Soifer, S.J., O'Keefe, J., Vu, T.-K.H., Charo, I.F., and Coughlin, S.R. (1992). Thrombin expression in normal and atherosclerotic human arteries. J. Clin. Invest. *90*, 1614–1621.
10. Griffin, C.T., Srinivasan, Y., Zheng, Y.-W., Huang, W., and Coughlin, S.R. (2001). A role for thrombin receptor signaling in endothelial cells during embryonic development. Science *293*, 1666–1670.
11. Even-Ram, S., Uziely, B., Cohen, P., Grisaru-Granovsky, S., Maoz, M., Ginzburg, Y., Reich, R., Vlodavsky, I., and Bar-Shavit, R. (1998). Thrombin receptor overexpression in malignant and physiological invasion processes. Nat. Med. *4*, 909–914.
12. Kamath, L., Meydani, A., Foss, F., and Kuliopulos, A. (2001). Signaling from protease-activated receptor-1 inhibits migration and invasion of breast cancer cells. Cancer Res. *61*, 5933–5940.
13. Hollenberg, M.D. (2000). Receptor binding and agonist efficacy: new insights from mutants of the thrombin protease-activated receptor-1 (PAR1). Mol. Pharmacol. *58*, 1175–1177.
14. Cook, J.J., Sitko, G.R., Bednar, B., Condra, C., Mellot, M.J., Feng, D.-M., Nutt, R.F., Shafer, J.A., Gould, R.J., and Connolly, T.M. (1995). An antibody against the exosite of the cloned thrombin receptor inhibits experimental arterial thrombosis in the African green monkey. Circulation *91*, 2961–2971.
15. Bernatowicz, M.S., Klimas, C.E., Hartl, K.S., Peluso, M., Allegretto, N.J., and Seiler, S.M. (1996). Development of potent thrombin receptor antagonist peptides. J. Med. Chem. *39*, 4879–4887.
16. Andrade-Gordon, P., Maryanoff, B.E., Derian, C.K., Zhang, H.-C., Addo, M.F., Darrow, A.L., Eckardt, A.J., Hoekstra, W.J., McComsey, D.F., Oksenberg, D., et al. (1999). Design, synthesis, and biological characterization of a peptide-mimetic antagonist for a tethered-ligand receptor. Proc. Natl. Acad. Sci. USA *96*, 12257–12262.
17. Covic, L., Gresser, A.L., Talavera, J., Swift, S., and Kuliopulos, A. (2002). Activation and inhibition of G protein-coupled receptors by cell-penetrating membrane-tethered peptides. Proc. Natl. Acad. Sci. USA *99*, 643–648.
18. Covic, L., Misra, M., Badar, J., Singh, C., and Kuliopulos, A. (2002). Pepducin-based intervention of thrombin receptor signaling and systemic platelet activation. Nat. Med. *8*, 1161–1165.
19. Kuliopulos, A., Covic, L., Seeley, S.K., Sheridan, P.J., Helin, J., and Costello, C.E. (1999). Plasmin desensitization of the PAR1 thrombin receptor: kinetics, sites of truncation, and implications for thrombolytic therapy. Biochemistry *38*, 4572–4585.
20. Chen, J., Ishii, M., Wang, L., Ishii, K., and Coughlin, S.R. (1994). Thrombin receptor activation. J. Biol. Chem. *269*, 16041–16045.
21. O'Brien, P.J., Prevost, N., Molino, M., Hollinger, M.K., Woolkalis, M.J., Woulfe, D.S., and Brass, L.F. (2000). Thrombin responses in human endothelial cells. Contributions from receptors other than PAR1 include the transactivation of PAR2 by thrombin-cleaved PAR1. J. Biol. Chem. *275*, 13502–13509.
22. Scarborough, R.M., Naughton, M., Teng, W., Hung, D.T., Rose, J., Vu, T.-K.H., Wheaton, V.I., Turck, C.W., and Coughlin, S.R. (1992). Tethered ligand agonist peptides. J. Biol. Chem. *267*, 13146–13149.
23. Bahou, W.F., Coller, B.S., Potter, C.L., Norton, K.J., Kutok, J.L., and Goligorsky, M.S. (1993). The thrombin receptor extracellular domain contains sites crucial for peptide ligand-induced activation. J. Clin. Invest. *91*, 1405–1413.
24. Bahou, W.F., Kutok, J.L., Wong, A., Potter, C.L., and Coller, B.S. (1994). Identification of a novel thrombin receptor sequence required for activation-dependent responses. Blood *84*, 4195–4202.
25. Nanevicz, T., Ishii, M., Wang, L., Chen, M., Chen, J., Turck, C.W., Cohen, F.E., and Coughlin, S.R. (1995). Mechanisms of thrombin receptor agonist specificity. J. Biol. Chem. *270*, 21619–21625.
26. Blackhart, B.D., Ruslim-Litrus, L., Lu, C.-C., Alves, V.L., Teng, W., Scarborough, R.M., Reynolds, E.E., and Oksenberg, D. (2000). Extracellular mutations of protease-activated receptor-1 result in differential activation by thrombin and thrombin receptor agonist peptide. Mol. Pharmacol. *58*, 1178–1187.

27. Ji, T.H., Grossmann, M., and Ji, I. (1998). G protein-coupled receptors: I. diversity of receptor-ligand interactions. J. Biol. Chem. *273*, 17299–17302.
28. Gerszten, R.E., Chen, J., Ishii, M., Ishii, K., Wang, L., Nanevicz, T., Turck, C.W., Vu, T.-K.H., and Coughlin, S.T. (1994). Specificity of the thrombin receptor for agonist peptide is defined by its extracellular surface. Nature *368*, 648–651.
29. Lerner, D.J., Chen, M., Tram, T., and Coughlin, S.R. (1996). Agonist recognition by proteinase-activated receptor and thrombin receptor. J. Biol. Chem. *271*, 13943–13947.
30. Al-Ani, B., Saifeddine, M., Kawabata, A., and Hollenberg, M.D. (1999). Proteinase activated receptor 2: role of extracellular loop 2 for ligand-mediated activation. Br. J. Pharmacol. *128*, 1105–1113.
31. Compton, S.J., Sandhu, S., Wisjesuriya, S.J., and Hollenberg, M.D. (2002). Glycosylation of human proteinase-activated receptor-2 (hPAR2): role in cell surface expression and signalling. Biochem. J. *368*, 495–505.
32. Palczewski, K., Kumasaka, T., Hori, T., Behnke, C.A., Motoshima, H., Fox, B.A., Trong, I.L., Teller, D.C., Okada, T., Stenkamp, R.E., et al. (2000). Crystal structure of rhodopsin: A G protein-coupled receptor. Science *289*, 739–745.
33. Rydel, T.J., Ravichandran, K.G., Tulinski, A., Bode, W., Huber, R., Roitsch, C., and Fenton, J.W. (1990). The structure of a complex of recombinant hirudin and human α-thrombin. Science *249*, 277–280.
34. Liu, L.W., Vu, T., Esmon, C.T., and Coughlin, S.R. (1991). The region of the thrombin receptor resembling hirudin binds to thrombin and alters enzyme specificity. J. Biol. Chem. *266*, 16977–16980.
35. Vu, T.-K.H., Wheaton, V.I., Hung, D.T., Charo, I., and Coughlin, S.R. (1991). Domains specifying thrombin-receptor interaction. Nature *353*, 674–677.
36. Ishii, K., Gerszten, R., Zheng, Y.W., Welsh, J.B., Turck, C.W., and Coughlin, S.R. (1995). Determinants of thrombin receptor cleavage. J. Biol. Chem. *270*, 16435–16440.
37. Mathews, I.I., Padmanabhan, K.P., Ganesh, V., Tulinsky, A., Ishii, M., Chen, J., Turck, C.E., Coughlin, S.R., and Fenton, J.W. (1994). Crystallographic structures of thrombin complexes with thrombin receptor peptides: existence of expected and novel binding modes. Biochemistry *33*, 3266–3279.
38. Jacques, S., LeMasurier, M., Sheridan, P.J., Seeley, S.K., and Kuliopulos, A. (2000). Substrate-assisted catalysis of the PAR1 thrombin receptor: enhancement of macromolecular association and cleavage. J. Biol. Chem. *275*, 40671–40678.
39. Ayala, Y.M., Cantwell, A.M., Rose, T., Bush, L.A., Arosio, D., and Cera, E.D. (2001). Molecular mapping of thrombin-receptor interactions. Proteins *45*, 107–116.
40. Ahn, H.-S., Foster, C., Boykow, G., Arik, L., Smith-Torhan, A., Hesk, D., and Chatterjee, M. (1997). Binding of a thrombin receptor tethered ligand analogue to human platelet thrombin receptor. Mol. Pharmacol. *51*, 350–356.
41. Matoukas, J.M., Panagiotopoulos, D., Keramida, M., Mavromoustakos, T., Yamdagni, R., Wu, Q., Moore, G.J., Saifeddine, M., and Hollenberg, M.D. (1996). Synthesis and contractile activities of cyclic thrombin receptor-derived peptide analogues with Phe-Leu-Leu-Arg motif: importance of the Phe/Arg relative conformation and the primary amino group for activity. J. Med. Chem. *39*, 3585–3591.
42. Jacques, S., and Kuliopulos, A. (2003). Protease-activated receptor-4 uses dual prolines and an anionic retention motif for thrombin recognition and cleavage. Biochem. J. *376*, in press.
43. Korepanova, A., Douglas, C., Leyngold, I., and Logan, T.M. (2001). N-terminal extension changes the folding mechanism of the FK506-binding protein. Protein Sci. *10*, 1905–1910.
44. Hammes, S.R., and Coughlin, S.R. (1999). Protease-activated receptor-1 can mediate responses to SFLLRN in thrombin-desensitized cells: evidence for a novel mechanism for preventing or terminating signaling by PAR1's tethered ligand. Biochemistry *38*, 2486–2493.
45. Mendre, C., Dufour, M.N., Roux, S.L., Seyer, R., Guillou, L., Calas, B., and Guillon, G. (1997). Synthetic rat V_{1a} vassopressin receptor fragments interfere with vasopressin binding via specific interaction with the receptor. J. Biol. Chem. *272*, 21027–21036.
46. Covic, L., Gresser, A.L., and Kuliopulos, A. (2000). Biphasic kinetics of activation and signaling for PAR1 and PAR4 thrombin receptors in platelets. Biochemistry *39*, 5458–5467.
47. Qui, X., Padmanabhan, K.P., Carperos, V.E., Tulinsky, A., Kline, T., Maraganore, J.M., and Fenton, J.W. (1992). Structure of the Hirulog 3 complex and nature of the S' subsites of substrates and inhibitors. Biochemistry *31*, 11689–11697.
48. Nakanishi-Matsui, M., Zheng, Y.-W., Sulciner, D.J., Weiss, E.J., Ludeman, M.J., and Coughlin, S.R. (2000). PAR3 is a cofactor for PAR4 activation by thrombin. Nature *404*, 609–613.
49. Kuliopulos, A., and Walsh, C.T. (1994). Production, purification, and cleavage of tandem repeats of recombinant peptides. J. Am. Chem. Soc. *116*, 4599–4607.
50. Brünger, A.T. (1987). X-PLOR: A System for X-Ray Crystallography and NMR (New Haven, CT: Yale University Press).
51. Hsu-Lin, S., Berman, C.L., Furie, B.C., August, D., and Furie, B. (1984). A platelet membrane protein expressed during platelet activation and secretion. J. Biol. Chem. *259*, 9121–9126.